Bioorganic & Medicinal Chemistry Letters 19 (2009) 5363–5367

Contents lists available at ScienceDirect

Bioorganic & Medicinal Chemistry Letters

journal homepage: www.elsevier.com/locate/bmcl

Discovery of 4*H*-pyrazolo[1,5-*a*]pyrimidin-7-ones as potent inhibitors of hepatitis C virus polymerase

Yongqi Deng [a,*], Gerald W. Shipps Jr. [a], Tong Wang [a], Janeta Popovici-Muller [a], Kristin E. Rosner [a], M. Arshad Siddiqui [a], Jose Duca [b], Alan B. Cooper [b], Michael Cable [b]

[a] *Schering-Plough Research Institute Cambridge, 320 Bent Street, Cambridge, MA 02141, United States*
[b] *Schering-Plough Research Institute, 2015 Galloping Hill Road, Kenilworth, NJ 07033, United States*

ARTICLE INFO

Article history:
Received 8 June 2009
Revised 24 July 2009
Accepted 28 July 2009
Available online 6 August 2009

Keywords:
Hepatitis C virus
Polymerase
Pyrazolopyrimidin-ones
Anti-viral agents

ABSTRACT

A series of 4*H*-pyrazolo[1,5-*a*]pyrimidin-7-one derivatives was synthesized and evaluated for inhibitory activity against HCV NS5B RNA-dependent RNA polymerase. A number of these compounds exhibited potent activity in enzymatic assay. The synthesis and structure–activity relationship are also described.

Hepatitis C virus (HCV) was identified in 1989 as the pathogen responsible for non-A and non-B hepatitis.[1] It has been estimated that 1–3% of the world's population is infected and is a leading cause of liver transplantation in the United States.[2] Because the virus often results in fibrosis and cirrhosis of the liver over a time course that can last decades, it is projected that the societal costs of this disease will increase over the next 20 years.[3] Current treatment options are limited, with interferon α-2b/ribavirin combinations having the most widespread application. Unfortunately this combination does not always produce sustained responses across all viral genotypes, particularly genotype 1. Therefore, the development of new inhibitors targeting HCV becomes urgent.

The HCV NS5B RNA-dependent RNA polymerase is a central enzyme in the replication of the virus and has been vigorously pursued by several groups.[4] Several nucleoside and non-nucleoside NS5B inhibitors have been previously described.[5,6] Recently we described the discovery and initial optimization of aminothiazole 5-carboxylic acid derivatives **1** as HCV polymerase inhibitors.[7] Significant enhancement of the potency of this series proved to be challenging. It was observed that the structure–activity relationship (SAR), specifically the requirement for cyclohexyl, was reminiscent of a series of inhibitors which bind to the 'finger-loop' region of NS5B.[8] This binding site is distinct from the previously-identified allosteric pocket that is occupied by compounds of either thiophene or phenylalanine scaffolds. Given the availability of a crystal structure for an inhibitor bound at the finger-loop site, molecular modeling was employed as part of consideration of alternative scaffolds and to rationalize observed SAR.

The improvement of intrinsic affinity through conformational constraints is well-documented,[9] and this prompted us to design a new inhibitor series with a more rigid skeleton. Several scaffolds were selected based on conformational analysis to see whether the hydrophobic groups and carboxylic acid could be projected into a similar orientation as in the aminothiazole series. One such scaffold was 4*H*-pyrazolo[1,5-*a*]pyrimidin-7-one (PPO), which possesses good pharmacokinetic properties and has been widely used in drug design (Fig. 1).[10]

Compound **2**, the PPO analog of **1**, was docked into the structure of NS5B using an induced-fit docking procedure[11] at the finger-loop binding site. The three 'anchors' of compound **2** in the NS5B finger-loop binding site—the carboxylate and neighboring phenyl

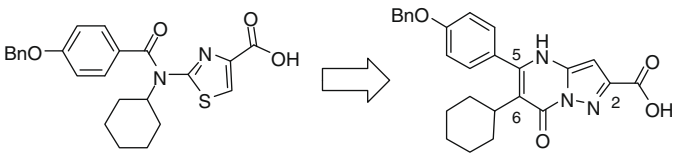

1 **2**

Figure 1. Design of pyrazolo[1,5-*a*]pyrimidin-7-one acid derivative **2** from aminothiazole **1**.

* Corresponding author. Tel.: +1 617 499 3516; fax: +1 617 499 3500.
E-mail address: yongqi.deng@spcorp.com (Y. Deng).

0960-894X/$ - see front matter © 2009 Elsevier Ltd. All rights reserved.
doi:10.1016/j.bmcl.2009.07.124

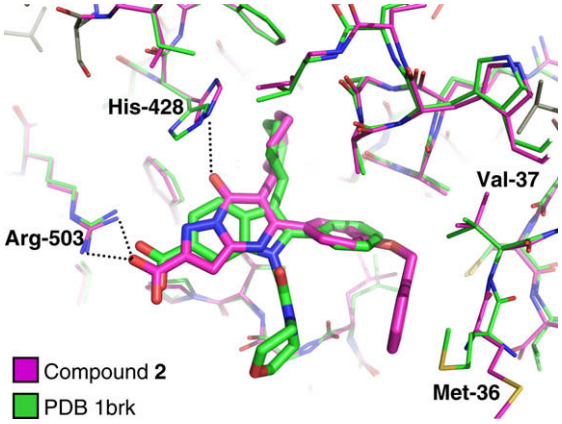

Figure 2. Overlay of the docked orientation of **2** (magenta) with the finger-loop inhibitor from the docking template structure (green; PDB 2brk). In addition to the hydrogen bond donors Arg-503 and His-428, residues are labeled where the sidechain orientation differs from the template resulting from the IFD procedure. The figure was produced using PyMOL (Warren L. DeLano *The PyMOL Molecular Graphics System*; DeLano Scientific: Palo Alto, CA, USA).

and cyclohexyl groups—overlay closely with their counterparts in the model template as well as other reported indoles and benzimidazoles[12] despite differences in scaffold and substitution (Fig. 2). To our surprise, the exocyclic oxygen atom of the PPO core was able to form a hydrogen bond interaction with the side chain of His-428. The unsubstituted N-4 position projects out of the binding pocket.

The IC_{50} value of **2** against HCV polymerase in the in vitro enzymatic assay was 1.4 μM, a fivefold improvement over **1**. Hereafter, we report the synthesis and optimization of a series of HCV polymerase inhibitors based on the 4*H*-pyrazolo[1,5-*a*]pyrimidin-7-one scaffold.

Two synthetic routes were developed in order to produce derivatives at C-5 and C-6 in a parallel manner. Scheme 1 depicts the general synthetic route which was used to make analogs at C-6. Reaction of the substituted acetophenone with diethyl carbonate in the presence of sodium hydride generated the corresponding β-ketone ester **3**, which then alkylated with alkyl bromide to produce α-substituted ketone ester **4**. The substituted ketone ester was then condensed with ethyl 5-amino-pyrazole-3-carboxylate in the presence of catalytic amount of *p*-toluene sulfonic acid in chlorobenzene to generate 6-substituted PPO ester **5**. Subsequent hydrolysis using aqueous lithium hydroxide in tetrahydrofuran (THF) produced the desired PPO carboxylic acid **6** in quantitative yield. Although analogs with various substitutions at C-5 can be made from this route, various ketones of interest are limited and this route is not optimal for large set of compounds. An alternative synthetic route was then developed to access analogs with various substitutions at C-5 and is highlighted in Scheme 2. In this synthetic route, the key intermediate α-substituted β-ketone ester **7** was generated in one step by reacting aryl substituted ethyl ace-

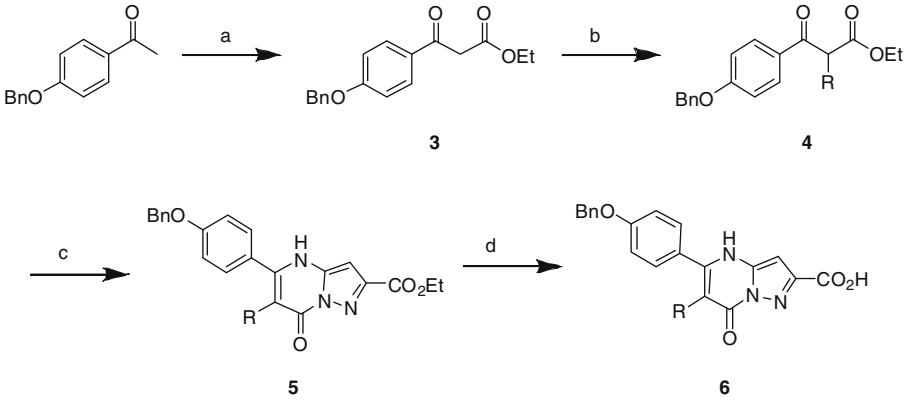

Scheme 1. Reagents and conditions: (a) diethyl carbonate, NaH, toluene, reflux, 16 h, 60–70%; (b) ArBr, KtBuO, EtOH; (c) 5-amino-2*H*-pyrazole-3-carboxylic acid ethyl ester, *p*-toluene sulfonic acid, chlorobenzene, 12 h, 110 °C, 30–70%; d: LiOH, THF, rt, 14 h, 95%.

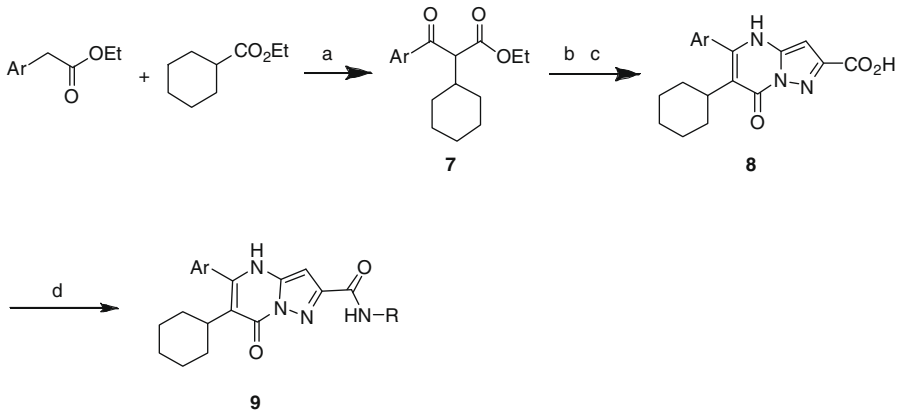

Scheme 2. Reagents and conditions: (a) NaH, DME, reflux; (b) 5-amino-2*H*-pyrazole-3-carboxylic acid ethyl ester, *p*-toluene sulfonic acid, chlorobenzene, 12 h, 110 °C, 30–70%; (c) LiOH, THF, rt, 14 h, 95%; (d) HATU, DIEA, rt, 2 h, 90%.

tate with ethyl cyclohexanecarboxylate in the presence of sodium hydride in dimethoxyethane (DME). The subsequent transformation was then carried out under the same condition as that described in Scheme 1 to give carboxylic acid **8** with various functional groups at C-5 position. Compounds that were further derivatized as amide **9** were prepared from acids generated from these schemes and the corresponding amines via amide couplings mediated by 2-(7-aza-1*H*-benzotriazole-1-yl)-1,1,3,3-tetramethyluronium hexafluorophosphate (HATU) in dimethylformamide (DMF) with *N*,*N*-diisopropylethylamine (DIEA).

To measure the efficacy of these compounds, a RNA polymerase assay was performed utilizing scintillation proximity assay (SPA) using radiolabeled GTP and a polyC/oligoG template/primer. Both Δ-55 and Δ-21 constructs of NS5B have been used according to a modified literature procedure.[13,14] Structure–activity relationship studies were carried out using both assays. In general, the potency of inhibitors using the Δ-21 construct was higher than using Δ-55 construct, which may suggest a perturbation of the binding environment. The rank order of IC_{50} values was similar between the two assays for early lower potency compounds; however the Δ-21 assay proved to be more discerning for higher potency compounds and ultimately this assay proved more informative.

The optimization began with an examination of substitution on the 6-position of the PPO scaffold. Our initial study indicated that an aryl group directly attached to C-6 was not tolerated as substitution at C-6 with a phenyl group resulted in a loss of activity. Subsequently, substitution at C-6 mainly focused on derivatives linked through an aliphatic carbon. In general, larger hydrophobic groups were preferred and resulted in compounds (**6b** and **6d**–**6g**) with moderate potency. This was consistent with the observation we made in the aminothiazole series. Introduction of an oxygen atom resulted compound **6c** with similar potency. Although the phenyl group was not tolerated when directly attached to the core, insertion of a carbon spacer resulted in compounds with moderate potency (**6k**–**6m**). The carbon spacer was also tolerated for the cyclohexyl group, as compound **6j** show comparable potency to the parent compound **2** while compound **6n** showed better activity in both assays. However, due to the poor solubility of compound **6n** and no significant improvement when compared to the parent compound **2**, we decided to maintain the cyclohexyl group at C-6 for subsequent analogs (Table 1).

Next, we investigated the substitutions on the C-5 position and the SAR is summarized in Table 2. Replacing the benzoxy with a methoxy group (compound **8a**), a phenoxy group (**c**ompound **8b**), a phenyl group (compound **8f**) or a benzyl group (compound **8g**) resulted in modest loss of potency compared to **2**. However, the distal phenoxy group substituted with either a methoxy or a trifluoro group resulted in compounds **8c** and **8d** with similar potency as **2**. Further increasing the hydrophobicity at C-5 by a substituted benzoxyl group in **2** led to small improvements in potency in compounds **8h**–**8j**. Interestingly, substitution at C-5 with small aromatic groups resulted in compounds (**8k** and **8l)** showing comparable potency in the Δ-55 assay, and some improvement in the Δ-21 assay compared to compound **2**. This SAR was distinct to this series of compounds and differed from the aminothiazole and similar compounds reported in the literature.[5,15]

The fact that the distal benzoxyl group is not necessary for this series of compounds enabled us to reduce the molecular weight of he scaffold. Initially, compound **8l** was used to explore the SAR for the carboxylic acid derivatives at the 2-position. Coupling the carboxylic acid of **8l** with simple amines generated corresponding amides with loss of activity. However, coupling **8l** with commercially available α-amino acids with various side chains generated compounds with improved potency and new SAR (Table 3). For example, the L-tyrosine derivative **9a** was found to be fourfold more potent than the corresponding D-tyrosine derivative **9b**.

Table 1
Modification of cyclohexyl group

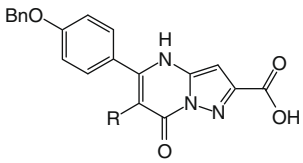

Compd	R	HCV NS5B Δ-55 IC_{50} (μM)	HCV NS5B Δ-21 IC_{50} (μM)
2		1.5 ± 0.1	1.0 ± 0.2
6a		>50	>12.5
6b		15 ± 1.1	9.5 ± 0.8
6c	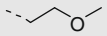	13 ± 0.9	3.7 ± 0.4
6d	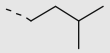	5.8 ± 1.2	1.5 ± 0.7
6e		>50	>12.5
6f	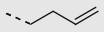	15 ± 1.0	6.7 ± 0.8
6g	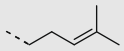	10 ± 0.4	3.5 ± 0.2
6h		8.8 ± 0.5	2.8 ± 0.3
6i		>12.5	10 ± 1.2
6j	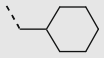	3.8 ± 0.4	0.4 ± 0.2
6k	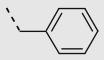	8.9 ± 0.6	4.2 ± 0.5
6l	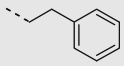	2.2 ± 0.6	1.2 ± 0.3
6m	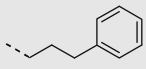	5.9 ± 0.3	2.5 ± 0.4
6n	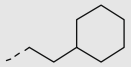	0.6 ± 0.3	0.17 ± 0.1

Removing a carbon from tyrosine gives 4-hydroxyphenylglycine analog **9c** with threefold less potency. Replacing the 4-hydroxylphenyl in tyrosine with an imidazole resulted in L-histidine analog **9d** with ninefold less potency. The most potent compound obtained from this round of optimization was tryptophan analog **9e**, which had an IC_{50} of 50 nM. The carboxylic acid functionality was found to be important as the corresponding methyl ester **9f**

Table 2
SAR at the distal hydrophobic group

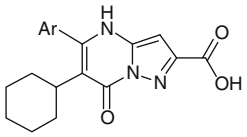

Compd	R	HCV NS5B Δ-55 IC_{50} (μM)	HCV NS5B Δ-21 IC_{50} (μM)
2	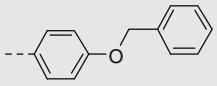	1.5 ± 0.1	1.0 ± 0.2
8a	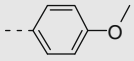	3.9 ± 0.2	n/a
8b	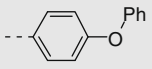	6.3 ± 1.2	n/a
8c	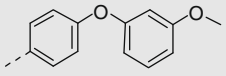	0.9 ± 0.1	n/a
8d	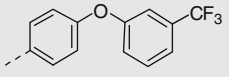	0.93 ± 0.03	n/a
8e	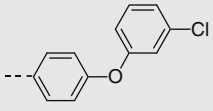	3.3 ± 0.03	n/a
8f	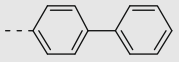	3.3 ± 0.3	3.1 ± 0.2
8g	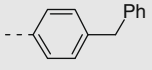	4.0 ± 0.5	2.6 ± 0.1
8h	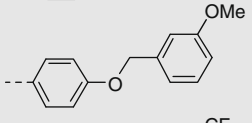	1.2 ± 0.1	1.0 ± 0.3
8i	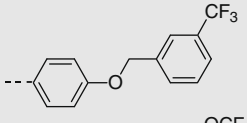	1.8 ± 0.1	0.9 ± 0.04
8j	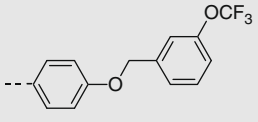	2.2 ± ± 0.1	1.5 ± 0.2
8k		2.3 ± 0.4	0.38 ± 0.2
8l		2.8 ± 0.1	0.29 ± 0.05
8m		6.4 ± 0.5	1.1 ± 0.3

Table 3

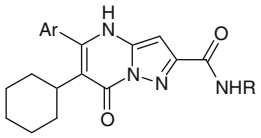

Compd	Ar	R	HCV NS5B Δ-21 IC_{50} (μM)
9a		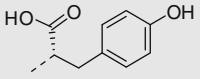	0.07 ± 0.01
9b		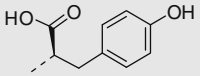	0.30 ± 0.03
9c		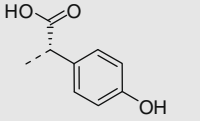	0.2 ± 0.01
9d		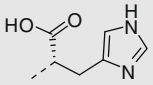	0.64 ± 0.02
9e		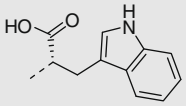	0.05 ± 0.01
9f		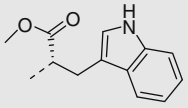	0.27 ± 0.05
9g		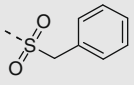	0.18 ± 0.01
9h		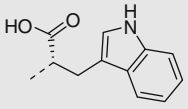	0.23 ± 0.04
9i		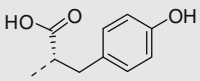	0.68 ± 0.05
9j		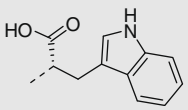	0.06 ± 0.01
9k		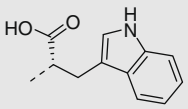	0.20 ± 0.03

showed fivefold loss of potency. The combination of tryptophan with different functional groups at C-5 position was also briefly explored. The position of the oxygen in the furan group showed little impact on the potency as 2-furanyl (compound **9e**) and 3-furanyl groups (compound **9j**) have similar potency. However, the corresponding thiophene shows fourfold loss of potency and similar results was observed for 3-fluorophenyl derivative **9h**. Consistent with the molecular model, the bioisosteric replacement of the C-2 carboxylate was tolerated as long as a hydrogen bond is maintained to the protein (Fig. 2). In fact, the solvent-accessibility of this group is consistent with the modest effect observed upon elaboration at this position.

The most potent inhibitors generated during this optimization study were subsequently tested in an HCV cell-based replicon assay of RNA replication.[16] Compound **9e**, despite its enzyme potency, had only weak potency in the cell-based assay (~50 μM), which led us to believe that this compound might have poor permeability likely due to the highly ionizable carboxylic acid group. Subsequent efforts have focused on replacing the carboxylic acid with bioisosteres to improve permeability. Moreover, substitution at unexplored solvent-exposed positions such as N-4 should afford modulation of physicochemical compound properties with little effect on intrinsic binding. Further efforts in this series and the results of cell permeability and activity in the cell-based assays, will be reported.

In conclusion, suitably substituted 4*H*-pyrazolo[1,5-*a*]pyrimidin-7-one analogs have been shown to be active against the NS5B RNA-dependent RNA polymerase. This series was obtained through conformational constraint of the previously reported aminothiazole series. Through the optimization of the 3, 5, and 2 positions, compounds with double digit nM potency in the in vitro enzymatic assay were obtained.

Acknowledgments

The authors would like to acknowledge Drs. B.A. Malcolm, B.M. Baroudy, and Charles Lesburg for insightful discussions.

References and notes

1. Choo, Q.-L.; Kuo, G.; Weiner, A. J.; Overby, L. R.; Bradley, D. W.; Houghton, M. *Science* **1989**, *244*, 359.
2. (a) Memon, M. I.; Memon, M. A. *J. Viral. Hepat.* **2002**, *9*, 84; (b) Poordad, F. F.; Tran, T.; Martin, P. *Exp. Opin. Emerg. Drugs* **2003**, *8*, 9.
3. (a) Hoofnagle, J. H. *Hepatology* **1997**, *26*, S15; (b) Wasley, A.; Alter, M. J. *Semin. Liver Dis.* **2000**, *20*, 1.
4. (a) Beaulieu, P. L.; Montse, L.-B. *Curr. Med. Chem. Anti-Infective Agents* **2002**, *1*, 163; (b) Tan, S.-L.; Pause, A.; Shi, Y.; Sonenberg, N. *Nat. Rev. Drug Disc.* **2002**, *1*, 867; (c) Adachi, T.; Ago, H.; Habuka, N.; Okuda, K.; Komatsu, M.; Ikeda, S.; Yatsunami, K. *Biochim. Biophys. Acta* **2002**, *1601*, 39.
5. (a) Koch, U.; Narjes, F. *Curr. Top. Med. Chem.* **2007**, *7*, 1302; (b) Carroll, S. S.; Olsen, D. B. *Infect. Dis. Drug Targets* **2006**, *6*, 17; (c) Koch, U.; Attenni, B.; Malancona, S.; Colarusso, S.; Conte, I.; Di Filippo, M.; Harper, S.; Pacini, B.; Giomini, C.; Thomas, S.; Incitti, I.; Tomei, L.; De Francesco, R.; Altamura, S.; Matassa, V. G.; Narjes, F. *J. Med. Chem.* **2006**, *49*, 1693; (d) Dragovich, P. S.; Blazel, J. K.; Ellis, D. A.; Han, Q.; Kamran, R.; Kissinger, C. R.; LeBrun, L. A.; Li, L.-S.; Murphy, D. E.; Noble, M.; Patel, R. A.; Ruebsam, F.; Sergeeva, M. V.; Shah, A. M.; Showalter, R. E.; Tran, C. V.; Tsan, M.; Webber, S. E.; Kirkovsky, L.; Zhou, Y. *Bioorg. Med. Chem. Lett.* **2008**, *18*, 5635; (e) Krueger, A. C.; Madigan, D. L.; Jiang, W. W.; Kati, W. M.; Liu, D.; Liu, Y.; Maring, C. j.; Masse, S.; McDaniel, K. F.; Middleton, T.; Mo, H.; Molla, A.; Montgomery, D.; Pratt, J. K.; Rockway, T. W.; Zhang, R.; Kempf, D. J. *Bioorg. Med. Chem. Lett.* **2006**, *16*, 3367; (f) Nittoli, T.; Curran, K.; Insaf, S.; DiGrandi, M.; Orlowski, M.; Chopra, R.; Agarwal, A.; Howe, A. Y. M.; Prashad, A.; Floyd, M. B.; Johnson, B.; Sutherland, A.; Wheless, K.; Feld, B.; O'Connell, J.; Mansour, T. S.; Bloom, J. *J. Med. Chem.* **2007**, *50*, 2108; (g) Habermann, J.; Capitò, E.; Ferreira, M. R. R.; Koch, U.; Narjes, F. J. *Bioorg. Med. Chem. Lett.* **2009**, *19*, 633; (h) Powers, J. P.; Piper, D. E.; Li, Y.; Mayorga, V.; Anzola, J.; Chen, J. M.; Jaen, J. C.; Lee, G.; Liu, J.; Peterson, M. G.; Tonn, G. R.; Ye, Q.; Walker, N. P. C.; Wang, Z. *J. Med. Chem.* **2006**, *49*, 1034.
6. (a) Beaulieu, P. L. *Curr. Top. Med. Chem.* **2007**, *8*, 614; (b) Koch, U.; Narjes, F. *Infect. Dis. Drug Targets* **2006**, *6*, 31.
7. Shipps, G. W.; Deng, Y.; Wang, T.; Popovici-Muller, J.; Curran, P. J.; Rosner, K. E.; Cooper, A. B.; Girijavallabhan, V.; Butkiewicz, N.; Cable, M. *Bioorg. Med. Chem. Lett.* **2005**, *15*, 115.
8. Di Marco, S.; Volpari, C.; Tomei, L.; Altamura, S.; Harper, S.; Narjes, F.; Koch, U.; Rowley, M.; De Francesco, R.; Migliaccio, G.; Carfi, A. *J. Biol. Chem.* **2005**, *280*, 29765.
9. (a) Ikegashira, K.; Oka, T.; Hirashima, S.; Noji, S.; Yamahaka, H.; Hara, Y.; Adachi, T.; Tsuruha, J.-I.; Doi, S.; Hase, Y.; Noguchi, T.; Ando, I.; Ogura, N.; Ikeda, S.; Hashimoto, H. *J. Med. Chem.* **2006**, *49*, 6950; (b) Hirashima, S.; Oka, T.; Ikegashira, K.; Noji, S.; Yamanaka, H.; Hara, Y.; Goto, H.; Mizojiri, R.; Nima, Y.; Noguchi, T.; Ando, I.; Ikeda, S.; Hashimoto, H. *Bioorg. Med. Chem. Lett.* **2007**, *17*, 3181.
10. (a) Senga, K.; Novinson, T.; Wilson, H. R. *J. Med. Chem.* **1981**, *24*, 610; (b) Selleri, S.; Bruni, F.; Costagli, C.; Costanzo, A.; Guerrini, G.; Ciciani, G.; Gratteri, P.; Bonaccini, C.; Aiello, Petra M.; Besnard, F.; Renard, S.; Costa, B.; Martini, Cla. *J. Med. Chem.* **2003**, *46*, 310.
11. The X-ray structure of an indole-based inhibitor that binds to the finger-loop region of NS5B (PDB access code: 2brk) was utilized as the frame of Ref. 8. In preparation for docking, all ligand and water molecules were deleted and hydrogen atoms were added and minimized using Macromodel as implemented in Maestro 8.5 (*Schrödinger, LLC, New York, NY, 2009*). Docking of **2** to NS5B was performed using Glide XP (Halgren, T. A.; Murphy, R. B.; Friesner, R. A.; Beard, H. S.; Frye, L. L.; Pollard, W. T.; Banks, J. L. *J. Med. Chem.* **2004**, *47*, 1750; Friesner, R. A.; Banks, J. L.; Murphy, R. B.; Halgren, T. A.; Klicic, J. J.; Mainz, D. T.; Repasky, M. P.; Knoll, E. H.; Shelley, M.; Perry, J. K.; Shaw, D. E.; Francis, P.; Shenkin, P. S. *J. Med. Chem.* **2004**, *47*, 1739.) An inner box region (the ligand midpoint remains within this box during docking) of 10 Å and outer box region of 24 Å were used. The induced-fit docking protocol (Sherman, W.; Day, T.; Jacobson, M. P.; Friesner, R. A.; Farid, R. *J. Med. Chem.* **2006**, *49*, 534), IFD, was used to perturb the initial NS5B model in the presence of the docked ligand **2**, while allowing a flexible adaptation of the protein environment upon compound binding. The IFD protocol consists of four steps: (1) softened-potential docking into the rigid receptor to generate an ensemble of poses; (2) sampling of protein conformations for each ligand pose generated in the first step; (3) redocking of the ligand into low energy induced-fit structures from the previous step; and (4) rescoring by accounting for the docking energy. Extra precision docking was used during the third and fourth steps (Glide XP (*Schrödinger, LLC, New York, NY, 2009*). All the options used during IFD were standard, as provided by the python interface in Maestro 8.5.
12. (a) De Francesco, R.; Carfí, A. *Adv. Drug Delivery Rev.* **2007**, *59*, 1242–1262; (b) Beaulieu, P. L. *Curr. Opin. Drug Disc. Dev.* **2006**, *9*, 618.
13. Briefly, 50 μL reactions containing 20 mM HEPES (pH 7.3), 7.5 mM DTT, 20 units/mL RNasIN, 0.5 μg/mL biotinylated oligoG_{12}, 5 μg/mL polyC, 0.5 μM GTP, 1 μCi/mL [^{3}H]-GTP, 10 mM $MgCl_2$, 60 mM NaCl, 100 μg/mL BSA, and 6 nM NS5B (Δ55) were incubated at room temperature for 50 min in 96-well plates with or without test compounds. Assay was terminated by the addition of 50 μL 10 mg/mL streptavidin-coated SPA beads supplemented with 100 mM EDTA, and the incorporation of labeled GTP determined by a TopCount Scintillation Counter. IC_{50} values were calculated from single experiments using 11 serial twofold dilutions (0.05–50 μM), and data were considered reliable only when the IC_{50} value of a positive internal control was within standard deviation range.
14. Assay was identical to that described in (9) except 5 μM GTP, 20 μCi/mL [^{3}H]-GTP, and 50 nM NS5B (Δ-21) enzyme form were used in a 3-h reaction at room temperature.
15. Ishida, T.; Suzuki, T.; Hirashima, S.; Mizutani, K.; Yoshida, A.; Ando, I.; Ikeda, S.; Adachi, T.; Hashimoto, H. *Bioorg. Med. Chem. Lett.* **2006**, *16*, 1859.
16. Lohmann, V.; Körner, F.; Koch, J. O.; herian, U.; Theilmann, L.; Bartenschlager, R. *Science* **1999**, *285*, 110.